

# $^1\text{H}$ assignment and secondary structure determination of human melanoma growth stimulating activity (MGSA) by NMR spectroscopy

Wayne J. Fairbrother<sup>a,\*</sup>, Dorothea Reilly<sup>b</sup>, Timothy Colby<sup>c</sup>, Richard Horuk<sup>c</sup>

<sup>a</sup>Department of Protein Engineering, <sup>b</sup>Department of Cell Culture, and <sup>c</sup>Department of Protein Chemistry, Genentech Inc., 460 Pt. San Bruno Blvd., South San Francisco, CA 94080-4990, USA

Received 28 July 1993

The solution structure of melanoma growth stimulating activity (MGSA) has been investigated using proton NMR spectroscopy. Sequential resonance assignments have been carried out, and elements of secondary structure have been identified on the basis of NOE, coupling constant, chemical shift, and amide proton exchange data. Long-range NOEs have established that MGSA is a dimer in solution. The secondary structure and dimer interface of MGSA appear to be similar to those found previously for the homologous chemokine interleukin-8 [Clowse et al. (1990) *Biochemistry* 29, 1689–1696]. The MGSA monomer contains a three stranded anti-parallel  $\beta$ -sheet arranged in a 'Greek-key' conformation, and a C-terminal  $\alpha$ -helix (residues 58–69).

Chemokines; Melanoma growth stimulating activity (MGSA); Protein structure; Nuclear magnetic resonance

## 1. INTRODUCTION

Melanoma growth-stimulatory activity (MGSA) is a mitogenic protein, initially identified as a factor secreted by the human melanoma cell line Hs294T [1]. The 73 amino acid residue protein corresponds to the gene product of the human *gro* gene [2]; the *MGSA/gro* gene is expressed by a variety of normal and transformed cell lines, including fibroblasts, melanoma cells, epithelial cells, and endothelial cells [2–5]. The polypeptide sequence of human MGSA indicates that it is a member of a family of chemotactic molecules known as chemokines [6,7] which includes platelet factor 4 (PF4),  $\beta$ -thromboglobulin ( $\beta$ -TB),  $\gamma$ -interferon induced protein ( $\gamma$ -IP10), and interleukin 8 (IL-8); these proteins can function as chemotactic factors for a variety of cells, as immune cell activators, and as regulators of cell growth [8].

When aligned according to their four cysteine residues the identity between MGSA and IL-8 is about 41% (Fig. 1), suggesting that the two proteins may share a similar polypeptide fold. Supporting this assumption is the fact that MGSA has been shown to compete with IL-8 for binding to neutrophil cell-surface receptors and has similar neutrophil chemotactic activity to IL-8 [9]; significant melanoma stimulating activity has also been observed for IL-8 [10]. More recently, however, studies using recombinant human MGSA have led to the identification of unique MGSA-specific receptors in human melanoma cells [11] and synovial fibroblasts [12]. MGSA binding to these sites could not be displaced by

IL-8, suggesting some significant structural (or dynamical) differences may exist between the two proteins. While high resolution structures of IL-8 have been determined both by NMR spectroscopy [13] and X-ray crystallography [14], to date no structural information has been obtained for MGSA. The present NMR studies were undertaken in order to obtain a detailed solution structure of MGSA, which, when compared with the existing solution and crystal structures of IL-8 should lead to an improved understanding of the mechanisms of action of these two important chemokines. As a necessary first step towards the determination of the solution structure of MGSA we have completed the proton resonance assignments and determined the protein's secondary structure based upon short-, medium-, and long-range NOEs, amide proton exchange data and  $^3J_{\text{HN}\alpha}$  coupling constants. The secondary structure of MGSA was found to be similar to that determined previously for IL-8 [13].

## 2. EXPERIMENTAL PROCEDURES

### 2.1. Preparation of MGSA

Expression and purification of recombinant human MGSA from *Escherichia coli* was as described previously [11] except that an additional FPLC purification step, using a phenyl superose column equilibrated at pH 7.7 with an ammonium sulfate gradient (1.8 to 0.7 M), was employed. The MGSA eluted at about 1.2 M ammonium sulfate. The pooled fractions were concentrated using Amicon Centriprep 10 concentrators and desalted using a Superose column. Following desalting the protein was again concentrated and washed several times with 45 mM potassium phosphate (pH 5.5, 90%  $\text{H}_2\text{O}/10\% \text{D}_2\text{O}$ ). The resulting NMR sample contained  $\sim 2.0$  mM protein at pH 5.7, and was judged pure by mass spectrometry. The  $\text{D}_2\text{O}$  sample used in this study was prepared by lyophilizing the 90%  $\text{H}_2\text{O}/10\% \text{D}_2\text{O}$  sample and dissolving in 99.996%  $\text{D}_2\text{O}$ .

\*Corresponding author. Fax: (1) (415) 225 3734.

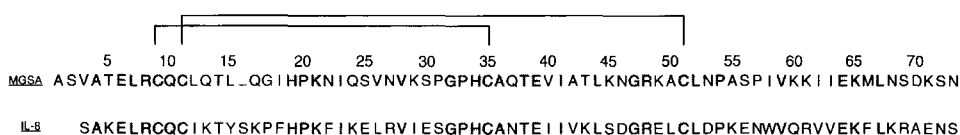


Fig. 1. Sequence alignment of human MGSA and IL-8. Conserved residues are indicated by shading.

## 2.2. NMR measurements

All NMR spectra were recorded on a Bruker AMX500 spectrometer. Spectra were acquired at either 30 or 20°C, and were referenced to internal 3-(trimethylsilyl)-propionic- $d_4$  acid. Standard pulse sequences and phase cycling were employed to record the following spectra: COSY [15], 2QF-COSY [16], pre-TOCSY-COSY [17], and double-quantum (2Q) [18,19]. TOCSY spectra [20,21], with spin-lock periods of 35 and 65 ms, were recorded using the 'clean' DIPSI-2rc sequence [22] for isotropic mixing. NOESY spectra [23,24] with mixing times of 50, 100, and 150 ms, and TOCSY spectra were acquired using a short pre-acquisition Hahn-echo period to improve the quality of the baseline [25,26]. Low-power phase-locked presaturation of the  $H_2O$  or residual HDO signal was used for all of the above experiments. In addition, a 150 ms NOESY spectrum was recorded in  $H_2O$  solution at 30°C using a jump-and-return read pulse [27]. All spectra were recorded in the phase-sensitive mode using time-proportional phase incrementation for quadrature detection in  $F_1$  [28-30].

$^3J_{HN\alpha}$  coupling constants were estimated from a COSY spectrum using the method of Kim and Prestegard [31]. Amide proton exchange with solvent was monitored at 30°C using a TOCSY spectrum, acquired immediately following dissolution of the lyophilized protein sample in  $D_2O$ . The total acquisition time for this spectrum was approximately one hour.

## 3. RESULTS

Sequential assignment of all the backbone  $^1H$  resonances and most of the side chain  $^1H$  resonances of MGSA has been achieved using conventional NOE-based assignment procedures [32,33]. COSY (pre-TOCSY-COSY in 90%  $H_2O$ /10%  $D_2O$  and 2QF-COSY in  $D_2O$ ), 2Q and TOCSY spectra of MGSA in both  $H_2O$  and  $D_2O$  solution were used for initial spin system identification, while NOESY spectra were used to identify sequential through-space connectivities. Most ambiguities were resolved by analysis of spectra acquired at two temperatures, 30 and 20°C. A summary of the sequen-

tial NOE data is given in Fig. 2, and the assignments obtained are listed in Table I.

The secondary structure of MGSA was determined from a qualitative analysis of the sequential NOE, amide proton exchange and  $^3J_{HN\alpha}$  coupling constant data summarized in Fig. 2, together with medium- and long-range NOE data involving  $C^\alpha H$  and backbone amide protons. The protein was found to contain a three-stranded anti-parallel  $\beta$ -sheet, characterized by stretches of strong sequential  $d_{\alpha N}(i, i+1)$  NOE connectivities, long-range backbone-backbone NOE connectivities [ $d_{NN}(i, j)$ ,  $d_{\alpha N}(i, j)$ , and  $d_{\alpha\alpha}(i, j)$ ], large  $^3J_{HN\alpha}$  coupling constants ( $> 8.5$  Hz), reduced amide proton exchange rates, and the  $C^\alpha H$  chemical shifts as analyzed according to the chemical shift index method of Wishart et al. [34]. A schematic representation of the  $\beta$ -sheet secondary structure is given in Fig. 3. The arrangement of the three strands in the anti-parallel  $\beta$ -sheet is that of a 'Greek key': strand 2 (residues 39-44) is hydrogen bonded to strands 1 (residues 25-29) and 3 (residues 48-52). Strands 1 and 2 are connected by a loop (residues 30-38), and strands 2 and 3 are connected by a  $\beta$ -hairpin. We note, however, that the sequential  $d_{NN}$  NOE connectivities indicated between residues Asn-46, Gly-47 and Arg-48 in Fig. 3 are ambiguous due to near degeneracy of the amide proton chemical shifts of residues Asn-46 and Arg-48 (Table I). A  $\beta$ -bulge, characterized by NOEs observed between the backbone amide proton of Gln-24 and Ser-25(NH), Leu-44( $C^\alpha H$ ), and Lys-45(NH), is also evident at the beginning of strand 1. In addition to the  $\beta$ -sheet structure, MGSA contains an  $\alpha$ -helix between residues 58-69, as characterized by the observed grouping of  $d_{NN}(i, i+1)$ ,  $d_{NN}(i, i+2)$ ,

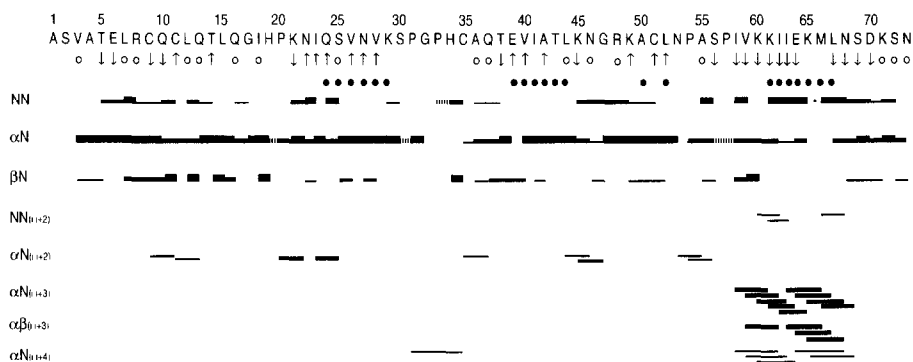


Fig. 2. Summary of the sequential NOE connectivities,  $^3J_{HN\alpha}$  and amide proton exchange data for MGSA. Sequential connectivities involving the  $C^\alpha H$  of proline residues are denoted by dashed lines. Measured  $^3J_{HN\alpha}$  coupling constants are indicated as follows:  $J < 7$  Hz ( $\downarrow$ );  $7 \text{ Hz} \leq J \leq 8.5$  Hz ( $\circ$ );  $J > 8.5$  Hz ( $\uparrow$ ). Slowly exchanging amide protons that are still present in a TOCSY spectrum recorded after dissolution of lyophilized protein in  $D_2O$  are indicated by closed circles.

Table I  
Proton resonance assignments of MGSA at 30°C, pH 5.7

Residue	NH	H $\alpha$	H $\beta$	H $\gamma$	H $\delta$	H $\epsilon$
Ala-1		4.16	1.57			
Ser-2		4.56	3.89, 3.89			
Val-3	8.28	4.16	2.08	0.93, 0.93		
Ala-4	8.41	4.31	1.40			
Thr-5	8.00	4.16	4.20	1.21		
Glu-6	8.38	4.29	2.04, 1.95	2.25, 2.21		
Leu-7	8.06	4.32	1.62, 1.48	1.57	0.85, 0.74	
Arg-8	7.87	4.78	2.08, 1.83	1.59, 1.59	3.20, 3.20	7.21
Cys-9	8.49	4.70	3.82, 2.72			
Gln-10	11.30	4.32	2.15, 2.01	2.39, 2.39		7.53, 6.87
Cys-11	9.48	4.94	3.18, 2.80			
Leu-12	8.69	4.38	1.69, 1.69	1.66	0.95, 0.88	
Gln-13	7.80	4.65	2.16, 2.03	2.35, 2.35		
Thr-14	8.49	4.56	3.98	1.08		
Leu-15	8.62	4.71	1.67, 1.67	1.83	0.94, 0.94	
Gln-16	8.77	4.48	2.22, 2.02	2.50, 2.50		7.56, 6.89
Gly-17	7.79	3.96, 3.81				
Ile-18	7.16	4.25	1.73	1.40, 1.12 (0.75) <sup>a</sup>	0.77	
His-19	8.54	4.79	3.09, 3.09		7.13	7.94
Pro-20		4.12	2.22, 2.08	2.03, 1.84	3.82, 3.28	
Lys-21	9.64	4.28	1.88, 1.84	1.38, 1.38	1.58, 1.54	2.88, 2.83
Asn-22	8.16	4.90	3.17, 2.79		7.52, 7.18	
Ile-23	7.66	3.92	1.96	1.68 (0.79)	0.72	
Gln-24	9.37	4.55	1.93, 1.76	2.31, 2.31		7.24, 6.86
Ser-25	8.22	5.38	4.03, 3.98			
Val-26	9.29	4.73	1.78	0.81, 0.79		
Asn-27	8.81	5.72	2.93, 2.61		7.22, 6.67	
Val-28	9.37	4.58	2.19	0.89, 0.83		
Lys-29	9.38	4.72	1.99, 1.75			
Ser-30	7.94	4.78	4.06, 4.06			
Pro-31		4.52	2.11, 1.81	2.02, 1.75	4.13, 3.62	
Gly-32	8.54	4.42, 4.07				
Pro-33		4.18	2.27, 1.43	1.98, 1.91	3.69, 3.59	
His-34	8.36	4.73	3.19, 2.92		7.12	8.15
Cys-35	7.20	4.75	3.02, 2.92			
Ala-36	8.86	4.51	1.48			
Gln-37	7.47	4.83	2.18, 1.99	2.44, 2.29		7.83, 6.72
Thr-38	8.69	4.54	3.97	1.13		
Glu-39	8.59	4.92	1.96, 2.00	2.45		
Val-40	9.56	4.92	2.29	0.85, 0.74		
Ile-41	9.16	4.73	1.83	1.55, 1.15 (0.82)	0.86	
Ala-42	9.88	5.31	1.37			
Thr-43	9.16	4.78	4.23	1.22		
Leu-44	9.42	5.07	2.16, 1.81	1.69	0.89, 0.73	
Lys-45	8.48	4.01	1.99, 1.83	1.39, 1.39	1.78, 1.78	2.93, 2.93
Asn-46	7.75	4.65	3.31, 2.83		7.44, 6.59	
Gly-47	8.14	4.34, 3.57				
Arg-48	7.76	4.36	1.94, 1.93	1.66, 1.60	3.21, 3.21	7.25
Lys-49	8.33	5.47	1.74, 1.60	1.50		2.97
Ala-50	9.16	4.71	1.27			
Cys-51	9.01	5.55	3.90, 3.13			
Leu-52	8.98	4.98	1.46, 1.44	1.68	0.79, 0.72	
Asn-53	8.86	4.81	2.99, 2.85		7.95, 7.15	
Pro-54		4.22			4.32, 4.10	
Ala-55	7.57	4.40	1.44			
Ser-56	7.68	4.90	4.22, 4.22			
Pro-57		4.38	2.51, 2.02	2.18, 2.18	4.20, 4.08	
Ile-58	7.65	3.89	1.96	1.57, 1.34 (0.97)	0.90	

Table 1 (continued)

Residue	NH	H $\alpha$	H $\beta$	H $\gamma$	H $\delta$	H $\epsilon$
Val-59	7.25	3.43	2.36	1.12, 0.85		
Lys-60	7.29	3.76	1.92, 1.90	1.55, 1.39	1.74, 1.71	3.01, 2.95
Lys-61	7.34	4.12	1.96	1.59, 1.50	1.69	2.98, 2.98
Ile-62	8.32	3.62	2.01	1.97, 0.97 (0.81)	0.78	
Ile-63	7.89	3.58	1.90	1.77, 1.03 (0.88)	0.74	
Glu-64	8.21	3.84	2.20, 2.09	2.47, 2.15		
Lys-65	8.01	4.14	1.98, 1.98			2.99, 2.99
Met-66	8.00	4.08	2.21, 1.96	2.87, 2.46		1.91
Leu-67	7.87	4.07	1.85, 1.69	1.95	0.87, 0.79	
Asn-68	7.55	4.80	2.97, 2.77		7.59, 6.92	
Ser-69	8.06	4.39	4.01, 3.97			
Asp-70	8.39	4.62	2.77, 2.69			
Lys-71	8.19	4.43	1.96, 1.82	1.49, 1.49	1.72, 1.72	3.05, 3.05
Ser-72	8.36	4.47	3.91, 3.91			
Asn-73	8.06	4.50	2.78, 2.71			

<sup>a</sup>Values in parentheses correspond to Ile C<sup>γ</sup>H<sub>3</sub>.

$d_{\alpha N}(i, i + 3)$ ,  $d_{\alpha\beta}(i, i + 3)$ , and  $d_{\alpha N}(i, i + 4)$  NOE connectivities, smaller  $^3J_{HN\alpha}$  coupling constants, reduced amide proton exchange rates (Fig. 2), and the C<sup>2</sup>H chemical shift index. The seven N-terminal residues and four C-terminal residues appear to be more flexible in solution, as evidenced by their significantly narrower linewidths and reduced NOE intensities.

Several medium-range NOEs involving residues 24–30, and observation of slowly exchanging amide protons for residues Val-26 and Val-28, are consistent with MGSA forming a dimer in solution. Strand 1 from the  $\beta$ -sheet in one monomer is hydrogen bonded in an anti-parallel fashion to the same strand in the other mono-

mer (Fig. 3), resulting in a contiguous six-stranded anti-parallel  $\beta$ -sheet. This evidence of dimer formation is consistent with the observation that MGSA did not penetrate the membrane of the Centriprep 10 concentrator, which has a nominal 10 kDa molecular mass cutoff, used during the protein purification procedure; the molecular mass of monomeric MGSA is  $\sim 7.9$  kDa.

#### 4. DISCUSSION

The secondary structure and dimer interface of MGSA are very similar to those reported previously for both IL-8 [13,14,35] and the two nominal dimeric units of PF4, which combine in solution to form a tetramer

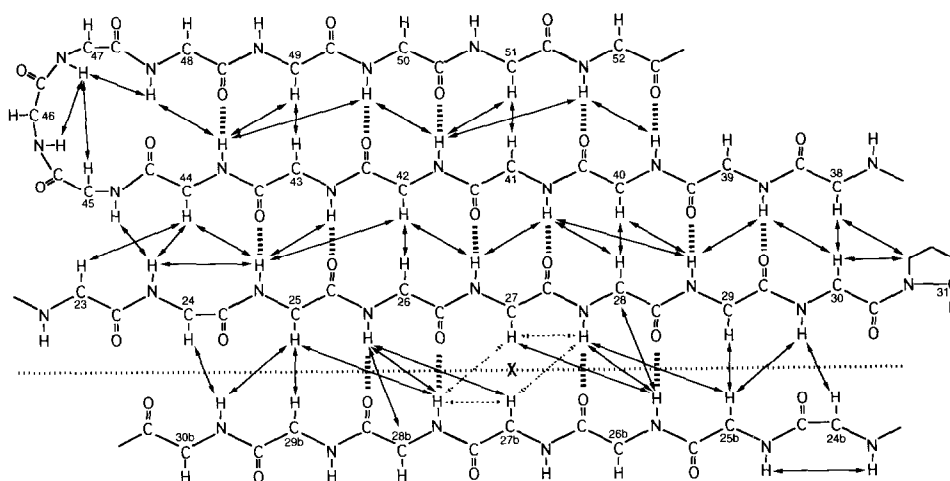


Fig. 3. Schematic representation of the anti-parallel  $\beta$ -sheet and dimer interface of MGSA as determined by analysis of NOE connectivities,  $^3J_{HN\alpha}$  coupling constants, and amide proton exchange data. Observed interstrand NOEs are indicated by arrows, and hydrogen bonds predicted from amide proton/solvent exchange and NOE data are indicated by thick broken lines. Dashed arrows correspond to observed NOEs which arise from both sequential and intermolecular connectivities. The dimer interface is indicated by a horizontal dashed line, while the dimer C<sub>2</sub> symmetry axis is indicated by an x.

[6]. The most significant difference between the structure of MGSA and IL-8 that can be determined from the current analysis is that the C-terminal  $\alpha$ -helix of MGSA appears to fray starting at residue Asp-70, rather than continuing to the C-terminal residue as found in IL-8 [35]. In this regard, MGSA appears similar to PF4, where the  $\alpha$ -helix was determined to end four residues from the C-terminus in the X-ray crystal structure [6]. The helices do, however, appear to start at the same relative positions (Ile-58 in the MGSA sequence) in the three proteins. A recent analysis of the backbone dynamics of IL-8 in solution [36] reveals that only residue 72 (the C-terminal residue) of the  $\alpha$ -helix is significantly more mobile than the remainder of the protein (excluding the N-terminal 6 residues). These data strongly support the original solution structure of IL-8 and suggest that the apparent differences between the C-terminal regions of IL-8 and MGSA are real.

A more detailed comparison of the structures of MGSA and IL-8 must await a full determination of the solution structure of MGSA. The dispersion of resonances in some regions of the NMR spectrum of MGSA (particularly the methyl region) is, however, relatively poor, due mainly to the lack of aromatic residues in the polypeptide sequence. This poor spectral dispersion might be expected to hinder the determination of a high resolution solution structure. With this in mind we have produced a  $^{15}\text{N}/^{13}\text{C}$  double-labeled MGSA sample and are proceeding with assignment and structure calculation, using the additional data derived from 3D and 4D heteronuclear edited NMR experiments.

*Acknowledgements:* We thank Dr. William Somers for assistance during protein purification, Dr. Beth Gillece-Castro for mass spectrometry analysis, and Dr. Nicholas Skelton for valuable discussion.

## REFERENCES

- [1] Thomas, H.G. and Richmond, A. (1988) *Mol. Cell Endocrinol.* 57, 69–76.
- [2] Anisowicz, A., Bardwell, L. and Sager, R. (1987) *Proc. Natl. Acad. Sci. USA* 84, 7188–7192.
- [3] Wen, D., Rowland, A. and Derynck, R. (1989) *EMBO J.* 8, 1761–1766.
- [4] Bordoni, R., Thomas, H.G. and Richmond, A. (1989) *J. Cell. Biochem.* 39, 421–428.
- [5] Richmond, A., Balentien, E., Thomas, H.G., Flagg, G., Barton, D.E., Spiess, J., Bordoni, R., Francke, U. and Derynck, R. (1988) *EMBO J.* 7, 2025–2033.
- [6] St. Charles, R., Walz, D.A. and Edwards, B.F.P. (1989) *J. Biol. Chem.* 264, 2092–2099.
- [7] Yoshimura, T., Matsushima, K., Tanaka, S., Robinson, E.A., Appella, E., Oppenheim, J.J. and Leonard, E. (1987) *Proc. Natl. Acad. Sci. USA* 84, 9233–9237.
- [8] Oppenheim, J.J., Zachariae, C.O., Mukaida, N. and Matsushima, K. (1991) *Annu. Rev. Immunol.* 9, 617–648.
- [9] Derynck, R., Balentien, E., Han, J.H., Thomas, H.G., Wen, D., Samantha, A.K., Zachariae, C.O., Griffin, P.R., Brachmann, R., Wong, W.L., Matsushima, K. and Richmond, A. (1990) *Biochemistry* 29, 10225–10233.
- [10] Matsushima, K. and Oppenheim, J.J. (1989) *Cytokine* 1, 2–13.
- [11] Horuk, R., Yansura, D.G., Reilly, D., Spencer, S., Bourell, J., Henzel, W., Rice, G. and Unemori, E. (1993) *J. Biol. Chem.* 268, 541–546.
- [12] Unemori, E.N., Amento, E.P., Bauer, E.A. and Horuk, R. (1993) *J. Biol. Chem.* 268, 1338–1342.
- [13] Clore, G.M., Appella, E., Yamada, M., Matsushima, K. and Gronenborn, A.M. (1990) *Biochemistry* 29, 1689–1696.
- [14] Baldwin, E.T., Weber, I.T., St. Charles, R., Xuan, J.-C., Appella, E., Yamada, M., Matsushima, K., Edwards, B.F.P., Clore, G.M., Gronenborn, A.M. and Wlodawer, A. (1991) *Proc. Natl. Acad. Sci. USA* 88, 502–506.
- [15] Aue, W.P., Bartholdi, E. and Ernst, R.R. (1975) *J. Chem. Phys.* 64, 2229–2246.
- [16] Rance, M., Sorensen, O.W., Bodenhausen, G., Wagner, G., Ernst, R.R. and Wüthrich, K. (1983) *Biochem. Biophys. Res. Commun.* 117, 479–485.
- [17] Otting, G. and Wüthrich, K. (1987) *J. Magn. Reson.* 75, 546–549.
- [18] Braunschweiler, L., Bodenhausen, G. and Ernst, R.R. (1984) *Mol. Phys.* 48, 535–560.
- [19] Rance, M. and Wright, P.E. (1986) *J. Magn. Reson.* 66, 372–378.
- [20] Bax, A. and Davis, D.G. (1985) *J. Magn. Reson.* 65, 355–360.
- [21] Braunschweiler, L. and Ernst, R.R. (1983) *J. Magn. Reson.* 53, 521–528.
- [22] Cavanagh, J. and Rance, M. (1992) *J. Magn. Reson.* 96, 670–678.
- [23] Bodenhausen, G., Kogler, H. and Ernst, R.R. (1984) *J. Magn. Reson.* 58, 370–388.
- [24] Kumar, A., Ernst, R.R. and Wüthrich, K. (1980) *Biochem. Biophys. Res. Commun.* 95, 1–6.
- [25] Davis, D.G. (1989) *J. Magn. Reson.* 81, 603–607.
- [26] Rance, M. and Byrd, R.A. (1983) *J. Magn. Reson.* 54, 221–240.
- [27] Plateau, P. and Guéron, M. (1982) *J. Am. Chem. Soc.* 104, 7310–7311.
- [28] Marion, D. and Wüthrich, K. (1983) *Biochem. Biophys. Res. Commun.* 113, 967–974.
- [29] Bodenhausen, G., Vold, R.L. and Vold, R.R. (1980) *J. Magn. Reson.* 37, 93–106.
- [30] Redfield, A.G. and Kuntz, S.D. (1975) *J. Magn. Reson.* 19, 250–254.
- [31] Kim, Y. and Prestegard, J.H. (1989) *J. Magn. Reson.* 84, 9–13.
- [32] Billeter, M., Braun, W. and Wüthrich, K. (1982) *J. Mol. Biol.* 155, 321–346.
- [33] Wüthrich, K. (1986) *NMR of Proteins and Nucleic Acids*, Wiley, New York.
- [34] Wishart, D.S., Sykes, B.D. and Richards, F.M. (1992) *Biochemistry* 31, 1647–1651.
- [35] Clore, G.M., Appella, E., Yamada, M., Matsushima, K. and Gronenborn, A.M. (1989) *J. Biol. Chem.* 264, 18907–18911.
- [36] Grasberger, B.L., Gronenborn, A.M. and Clore, G.M. (1993) *J. Mol. Biol.* 230, 364–372.